Journal of Applied Sciences and Nanotechnology

Journal homepage: jasn.uotechnology.edu.iq

Mechanisms, Performance Enhancements, and Scalability Prospects of Solvent-Annealed Perovskite Solar Cells: A Review

[1,2]Ammar Abdullah Hamad Al-Janabi*, [2]Chtourou R.

[1]Higher School of Science and Technology of Hammam Sousse, The University of Sousse, Tunisia
[2]Nanomaterials and Systems for Renewable Energy Laboratory, Research and Technology Center of Energy, Technoparc Borj Cedria, BP 095, Hammam Lif, Tunisia

A R T I C L E I N F O

Article history:
Received: June, 01, 2025
Accepted: August, 02, 2025
Available online: September, 10, 2025

Keywords:
Solvent annealing,
Perovskite solar cells,
Grain growth and morphology,
Scalability challenges

Corresponding Author:
Ammar Abdullah Hamad Al-Janabi
ammar.a.hamad@uotechnology.edu.iq

A B S T R A C T

Perovskite solar cells have rapidly advanced due to their exceptional optoelectronic properties, but achieving uniform crystallization and stability remains challenging. This review examines solvent-assisted annealing, including solvent-vapor and anti-solvent treatments as a strategy to modulate perovskite crystallization for enhanced device performance. Solvent vapors (e.g. DMF, DMSO, alcohol mixtures) introduced during thermal annealing sustain a supersaturated environment that extends nucleation and enables Ostwald ripening, yielding markedly larger grain sizes and improved crystallinity. Studies show that solvent annealing can increase MAPbI3 carrier diffusion lengths beyond 1 μm and maintain >14.5% efficiency even for films up to 1 μm thick. Advanced schemes, such as combined DMSO-water vapor annealing, have produced nearly single-crystal grains and devices with 19.5% power conversion efficiency (PCE), by reducing defect-mediated recombination. These microstructural gains translate into higher PCE and stability: solvent-annealed films exhibit fewer trap sites and inhibited moisture degradation. Finally, we address scalability: ambient solvent-antisolvent treatments have yielded >5 μm grains with 100% film coverage in large-area Perovskite solar cells. Overall, solvent annealing emerges as a powerful tool for tailoring perovskite films. This review synthesizes the mechanisms and performance benefits of solvent annealing and evaluates its prospects for scalable, industrialized PSC fabrication. By identifying key challenges and emerging solutions, it aims to guide future research efforts toward more efficient and manufacturable perovskite solar technologies.

https://doi.org/10.53293/jasn.2025.7711.1347, Department of Applied Sciences, University of Technology - Iraq.

1. Introduction

Solar photovoltaics (PV) are now widely recognised as a key technology for addressing climate change and meeting rising energy demand. Solar power has consistently emerged as one of the most promising, reliable, and renewable energy sources [1]. Traditional silicon PV dominates the market due to its high efficiency and reliability, but its performance is approaching its theoretical Shockley-Queisser limit (33.7%) [2]. Emerging thin-film PV

technologies promise further improvements in cost and functionality. In just over a decade, metal-halide perovskite solar cells (PSCs) have surged from first demonstrations (3.8% efficiency in 2009 [3]) to certified records exceeding 26%. Moreover, perovskite-silicon tandem cells have reached >33% [1, 2], surpassing the single-junction limit for silicon. These efficiency advances have been reported in periodic reviews, and the NREL efficiency chart shown in **Fig. 1** illustrates a unique aspect of PSC research with unprecedented improvement speed, often termed the fastest of any PV technology [4]. These rapid gains are driven by halide perovskites' exceptional optoelectronic properties (strong visible absorption, long carrier diffusion lengths, and tuneable bandgap) and their compatibility with low-temperature, solution-based fabrication [5, 6]. Crucially, PSCs are composed of earth-abundant elements and can be processed by roll-to-roll or inkjet methods [5, 7], offering the prospect of terawatt-scale, low-cost production. Industry adoption is already beginning: companies such as Oxford PV and others have announced commercial perovskite-silicon tandem modules with power conversion efficiency (PCE) of 24% [2]. In short, perovskite photovoltaics have emerged as a most promising next-generation solar technology that could complement or even rival silicon-based PV in large-scale applications [1].

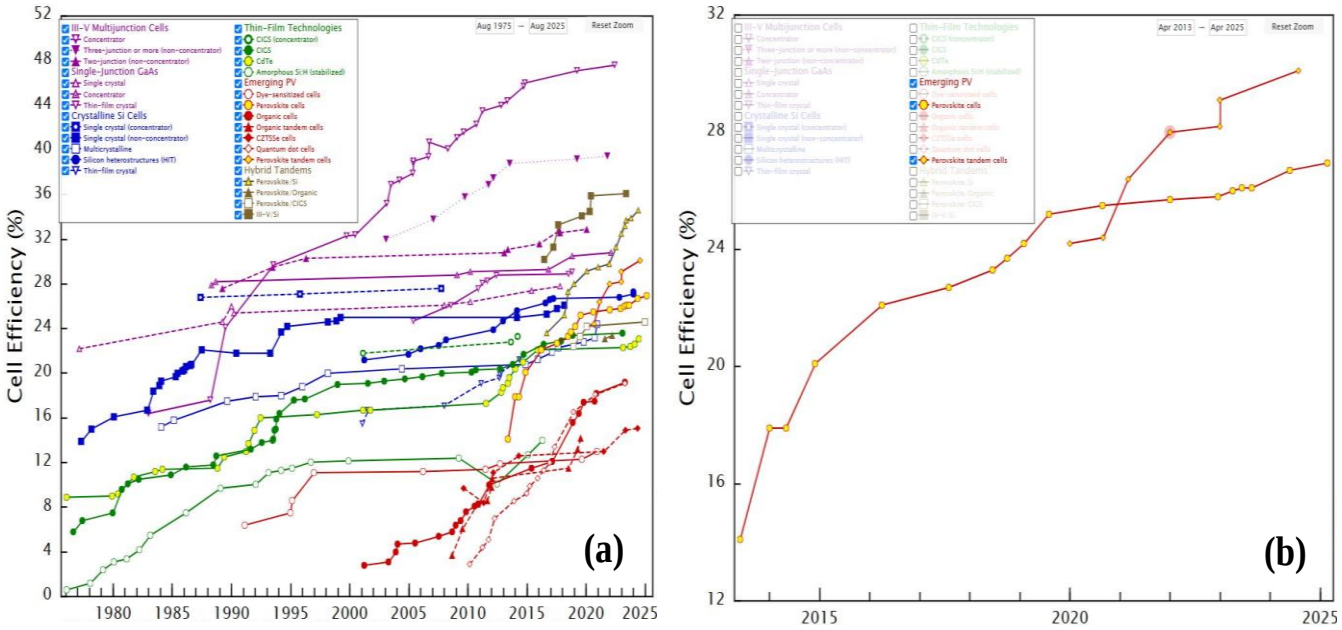

Figure 1: a) NREL chart with all verified solar cell types, and **b**) only verified perovskite solar cells [4].

Despite this impressive rise, PSCs still face significant challenges. Film quality and device stability remain key obstacles to reliable performance. The perovskite absorber is typically cast from solution (e.g. by spin-coating, blade or slot-die coating) and then annealed to crystallize the film [8–10]. The morphology of the resulting polycrystalline film: grain size, coverage, and defect density directly control efficiency and hysteresis. Laboratory best-efficiency cells rely on careful solvent control. For example, rapid removal of solvents via anti-solvent dripping (e.g. toluene or chlorobenzene wash) has been the standard approach to induce fast nucleation and smooth, pinhole-free films. Alternative physical methods (hot-casting, gas-blowing, vacuum-assisted quenching) have also been explored to accelerate drying and improve film quality. Chemical additives (e.g. chlorine or hypophosphite salts) and solvent engineering (mixed solvents, Lewis-base adducts) likewise play crucial roles in slowing crystallization to favor larger grains and passivate defects. Even so, such techniques that work on small cells (0.1 cm^2) often fail when scaling up. Large-area modules (>800 cm^2) show much lower PCE, largely due to difficulty in obtaining uniform film coating over meter-scale areas [7]. Several reports note an efficiency gap between lab-scale and commercial-scale devices [2, 7]. The low activation energy of perovskite crystallization facilitates flexible deposition, but also implies that uncontrolled solvent dynamics lead to inhomogeneity on large substrates [7]. Thus, understanding crystallization kinetics and developing robust, scalable film deposition techniques are vital for advancing PSCs toward commercialization.

Among strategies to improve perovskite film formation, solvent annealing (or solvent-vapor annealing, SVA) has

attracted obvious interest. In this post-deposition treatment, a partially dried perovskite film is exposed to a saturated vapor of a solvent, typically the same polar aprotic solvent used in the precursor (e.g. DMF or DMSO or other solvents) while heating. The solvent vapor temporarily plasticizes the film, providing a humid environment that promotes controlled crystal growth and Ostwald ripening. This approach is analogous to solvent-vapor annealing in polymer thin films, where vapor ingress swells the film and alters microstructure. Xiao *et al.* pioneered SVA in perovskites, showing that DMF vapor annealing of a two-step $MAPbI_3$ film dramatically enlarged the grains. Their annealed films exhibited lateral grain sizes up to 1 μm and carrier diffusion lengths >1 μm, enabling very efficient thick-film devices (PCE = 15.6%). Crucially, they found that efficiency remained above 14.5% even when film thickness increased from 250 nm to 1 μm [11], underscoring SVA's utility for high-absorption layers. Liu *et al.* then introduced alcohol-vapor annealing (using methanol or ethanol), which selectively dissolves the organic halide component. The alcohol vapor "heals" pinholes and effectively passivates defects (by redistributing MAI), yielding compact, defect-suppressed films [12]. Cao *et al.* reported a related mechanism: residual solvent molecules in the lattice drive Ostwald ripening. By adjusting annealing time and temperature, they obtained large columnar grains with minimal small-crystal precursors [13]. In each case, SVA-treated films delivered higher device fill-factor and sometimes higher open-circuit voltage, translating to clear PCE gains. For example, implementing methanol SVA raised PSC efficiency into the mid-teens [14]. Overall, solvent-annealed films show excellent grain quality improvements and greater potential for efficiency improvements compared to films annealed by heat only [15].

Notably, solvent annealing is versatile: it can be applied to one-step and two-step processes, as well as for planar or mesoscopic device structures, and mixed-cation perovskites. Choosing a specific solvent (DMF, DMSO, or mixed/aqueous vapors) and annealing duration critically affects the final material properties. For instance, high vapor concentration can over-dissolve the film and degrade the open-circuit voltage (Voc) [16]. Some groups, therefore, employ mild, room-temperature vapor environments or mixed solvent vapors to gently modulate crystallization. Recent work on wide-bandgap perovskites, e.g. FA/Cs-$Pb(I, Br)_3$, shows that SVA can offset issues from additives: Yu *et al.* combined $Pb(SCN)_2$ additive with DMF vapor annealing to enlarge grains from 60 nm to >1000 nm and extend performance lifetimes by 3 times, boosting PCE of $FA_{0.8}Cs_{0.2}Pb(I_{0.7}Br_{0.3})_3$ cells from 13.4% to 17.7% [17]. Such reports highlight that solvent annealing can synergize with other film-engineering methods.

Despite these successes, many questions remain unsolved. Fundamental mechanisms of SVA, such as solvent-perovskite interactions, vapor diffusion kinetics, and nucleation pathways, are still under investigation. For example, it is not fully understood how different solvents (polar aprotic vs. alcohol vs. water) influence intermediate phases and defect chemistry. The optimal SVA protocol (solvent choice, vapor pressure, temperature, time) likely depends on perovskite composition and device structure, yet systematic studies are scarce. Crucially, the long-term stability implications of SVA are uncertain: while larger grains may reduce defect density, residual solvent or altered grain boundaries might affect moisture resistance. Scalable implementation is another open issue. Unlike antisolvent dripping (which is inherently batch-scale), vapor treatments must be integrated into continuous coating processes. Achieving uniform solvent vapor exposure across large substrates or roll-to-roll webs is non-obvious. Thus, for industrial relevance, the scalability prospects of SVA must be carefully assessed.

By adjusting solvent vapor conditions, it is possible to modify perovskite morphology, which can surpass the capabilities of thermal annealing alone. However, to fully realize its potential, key research gaps must be addressed: elucidating the crystal growth mechanisms under SVA, optimizing protocols for diverse perovskite formulations, and demonstrating SVA in large-area manufacturing contexts. The present review surveys these aspects, focusing on the mechanisms, performance enhancements, and scalability prospects of solvent-annealed perovskite solar cells. This review aims to guide future efforts by identifying critical challenges and opportunities in this evolving field.

Unlike previously published reviews, this work introduces a comprehensive overview of both fundamental mechanisms and industrial implications of solvent annealing for perovskite solar cells. Over 50 recent studies from 2022–2024 have been analysed in this review, and a comparative evaluation of annealing protocols and scalability bottlenecks that have not been thoroughly explored in earlier literature.

2. Fundamentals of Perovskite Film Formation

Metal-halide perovskite films form via solution processing and crystallisation into a polycrystalline semiconductor layer. The morphology (grain size, coverage, defect density) of these films is crucial for solar cell performance, as non-uniform or defect-ridden films cause carrier recombination and hysteresis. Achieving uniform, high-quality perovskite films on large areas remains a big challenge for scaling up production [18]. Film formation involves multiple stages: solvent evaporation, nucleation of perovskite crystals, growth, and coalescence of grains, all of which must be carefully controlled to optimise device efficiency.

2.1 Nucleation and Crystal Growth

In solution-deposited $CH_3NH_3PbI_3$ ($MAPbI_3$) and mixed-cation perovskites, crystallization typically proceeds via heterogeneous nucleation on the substrate [18]. According to classical nucleation theory, the rate of nucleus formation depends on factors like supersaturation, temperature, and interface energy. Therefore, according to Young's equation and Thomson-Gibbs equation [19], the specific expression of the heterogeneous nucleation energy barrier can be expressed as follows **Eq. (1)** [20]:

$$\Delta G_{hetero} = \frac{16\pi\sigma^3\vartheta^2}{3\Delta\mu^2} \times \frac{2-3\cos\theta+\cos^3\theta}{4} \quad (1)$$

where: ΔG_{hetero} is the energy barrier of heterogeneous nucleation, υ is the critical nucleus volume, θ is the contact angle between solution and substrate, Δμ is the chemical potential difference between the precipitated crystal and the mother liquid, and σ is the interface energy between the solution and the substrate. Therefore, the nucleation rate can be expressed in **Eq. (2)** [20]:

$$\frac{dN_{hetero}}{dt} = \Gamma exp\left[\frac{-\Delta G_{hetero}}{k_B T}\right] = \Gamma exp\left[\frac{-16\pi\sigma^3\vartheta^2}{3k_B T\Delta\mu^2} \times \frac{2-3\cos\theta+\cos^3\theta}{4}\right] \quad (2)$$

Where: N_{hetero} is the heterogeneous nucleation rate, t is the time, T is the temperature, k_B is the Boltzmann constant, and Γ is the Zeldovich factor. Once the nucleus is formed, the growth begins spontaneously (assuming that the size of the formed crystal nucleus is uniform). According to McCabe's law, the total crystal growth rate can be expressed as follows **Eq. (3)** [19]:

$$R = \frac{d\Delta C}{dt} \quad (3)$$

where: R is the total crystal growth rate, t is the time, and ΔC is the supersaturation concentration of the solution. In practice, controlling the balance between initial nucleation and subsequent crystal growth is key. Rapid *nucleation* coupled with slower *crystal growth* produces dense, uniform films with large grains [21]. This paradigm is often summarised as "fast nucleation and slow crystallisation" being essential for high-quality perovskite films [21]. For example, anti-solvent quenching (dripping a poor solvent during spin-coating) induces an abrupt supersaturation that generates a burst of nuclei, yielding full film coverage and eliminating pinholes [22]. Conversely, allowing the wet film to dry more slowly (or under solvent vapour) favours the growth of fewer nuclei into larger crystals. An Ostwald ripening process can occur during thermal annealing, wherein small crystallites dissolve and redeposit onto larger grains, further coarsening the film [7]. The optimal strategy is often a two-step process: first, lock in a network of crystallites to avoid voids, then allow grain growth to improve crystallinity [21]. Spin coating protocols use a carefully timed anti-solvent step to induce immediate nucleation, followed by thermal annealing to enable crystal growth [7, 22]. **Fig. 2** shows the chemical reaction between PbI_2 and the organic halides for nucleation and crystal growth stages.

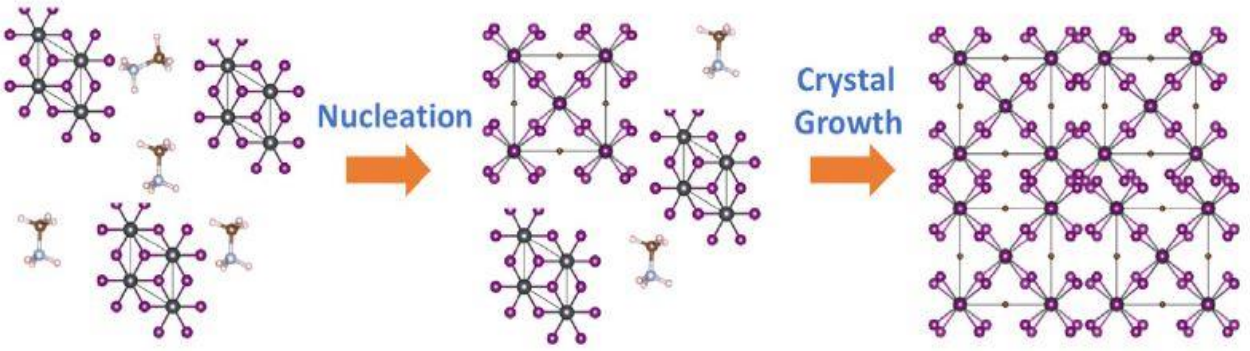

Figure 2: The schematics of the chemical reaction between PbI_2 and the organic halides for nucleation and crystal growth [23].

2.2 Solvent Coordination and Intermediate Phases

Unlike classical semiconductors, perovskite precursors can form solvated intermediate phases that strongly influence film formation. Polar aprotic solvents such as dimethylformamide (DMF) and dimethyl sulfoxide (DMSO) coordinate with PbI_2 to form adducts in solution [22]. The intermediate phase is formed due to the O-donor Lewis base properties of the polar aprotic solvents, and the strong Lewis basicity favors the formation of a phase(s) with AX, PbI_2, KCl, NH_4Cl [24]. As the solution dries, these solvent-lead complexes (e.g. the MA2Pb3I_8.2DMSO phase in $MAPbI_3$) precipitate first [25]. Upon heating, the intermediate converts into the perovskite phase, releasing the coordinated solvent. This two-step crystallization (intermediate → perovskite) assists in regulating crystal growth: the intermediate holds the precursors in a network, preventing rapid, uncontrolled crystallization [7]. For example, the use of a mixed DMF/DMSO solvent leads to a transient DMSO-adduct phase that slows down $MAPbI_3$ crystal formation and yields more uniform, dense films [26]. The precise chemistry of these intermediates depends on the precursors and additives. Additives like chloride or thiocyanate can introduce alternate intermediate phases or modify solubility, further tuning the crystallization pathway [27]. Overall, solvent coordination chemistry has emerged as a universal strategy to control perovskite film morphology [28].

2.3 Grain Growth, Boundaries and Defects

The as-formed perovskite films consist of numerous crystal grains separated by grain boundaries (GBs). Electronically, these GBs are sensitive regions that often harbor traps or vacancies and can impede charge transport [29, 30]. Rapid crystallization (e.g. excessive nuclei) tends to produce many small grains, increasing total GB area and defect density [29, 31]. By contrast, larger grain sizes are generally associated with improved electronic quality, where charge carriers can move longer distances without encountering a GB, and the overall surface defects are reduced. Notably, hot-casting methods that grow millimeter-scale grains have achieved hysteresis-free solar cells, attributing the stability to reduced bulk defects and improved carrier mobility in the large-grain films [31]. Grain boundaries in perovskites are dynamic: at moderate annealing temperatures, halide ions and vacancies are mobile and can redistribute, leading to partial “healing” or coalescence of grains over time [32, 33]. This is a double-edged sword; while some GBs anneal out (reducing trap-assisted recombination), ion migration can also induce new defects or phase segregation under bias and illumination. Thus, researchers employ passivation strategies (e.g. polymer or ionic coatings, additive diffusion) to chemically passivate GB defects [29, 32]. From a device physics perspective, grain boundaries and defects act as non-radiative recombination centers that diminish open-circuit voltage and fill factor if not controlled [30]. Effective film formation aims to minimize deep traps (like under-coordinated Pb or halide vacancies) and ensure GBs are benign or even beneficial. For instance, a small excess of PbI_2 often remains at GBs, which can passivate under-coordinated Pb sites, but excessive PbI_2 or other secondary phases will affect device performance [29, 30]. The careful balance between grain growth and defect passivation is essential to perovskite film fabrication.

2.4 Influence of Precursor Chemistry

The composition of the perovskite precursor (the A-site cation mixture, halide ratio, and any additives) strongly affects the crystallisation behaviour. $MAPbI_3$ (the archetypal perovskite) crystallises in a tetragonal phase at room

temperature, whereas $FA_{0.85}Cs_{0.15}Pb(I_{0.85}Br_{0.15})_3$ (a common triple-cation formulation) crystallises in a cubic phase with improved phase stability. Formamidinium lead iodide ($FAPbI_3$) has a small formation energy difference between its photoactive black alpha-phase and a yellow hexagonal delta-phase; as a result, films of $FAPbI_3$ often require high-temperature annealing or compositional tuning to avoid the undesirable delta-phase. Mixing methylammonium (MA^+) or caesium into $FAPbI_3$ assists in stabilising the black phase and yields films with fewer phase impurities. Saliba *et al.* showed that a MA/FA/Cs triple-cation perovskite is less sensitive to processing conditions, producing highly reproducible films and devices. The triple-cation films had reduced trap densities and remained phase-pure over a range of annealing temperatures, in contrast to single-cation perovskites [34]. In general, larger A-cations like formamidinium (FA) reduce the crystallisation kinetics (due to stronger hydrogen bonding and different solvent interactions) compared to MA, often resulting in different grain structures. Inorganic cations (Cs, Rb) can also influence crystallisation: Cs^+ tends to reduce the lattice parameter and can promote more monolithic grain growth, while rubidium has been reported to induce highly crystalline FA-based perovskites without the need for bromide or MA, improving both grain quality and stability [35]. In addition to the A-site, the selection of halides and additives also plays a critical role. Incorporating a small fraction of bromide into iodide perovskites (for instance, forming $MAPb(I_{1-x}Br_x)_3$ can slightly widen the bandgap but also modify crystallisation by changing the solubility and crystallographic kinetics. Additives such as methylammonium chloride (MACl) or lead thiocyanate ($Pb(SCN)_2$) are famous for enlarging grain size and improving surface coverage [27, 36]. MACl, for example, was found to induce the formation of a transient $MAPbI_3$.MACl intermediate that slowed crystal growth and eventually yielded perovskite grains six times larger than the used control [27]. Such chemical additives can passivate charged defects as well, by either incorporating into the crystal or by modifying the grain boundary chemistry [27, 36].

3. Overview of Annealing Techniques

After deposition of the perovskite wet film, a subsequent annealing step is mostly required to crystallize the perovskite and optimize its microstructure. Conventional thermal annealing (heating the film on a hotplate or in an oven at 100°C for 10-30 minutes), illustrated in **Fig. 3**, serves to evaporate residual solvent and induce the conversion of any intermediate phases into the perovskite crystal structure [7]. However, simple thermal annealing often provides limited control over crystallization kinetics. In recent years, a variety of advanced annealing techniques have been developed to manipulate the nucleation and growth of perovskite films, thereby improving grain size, film uniformity, defect passivation, and even scalability [21]. Broadly, these techniques include solvent annealing (exposing the film to solvent vapors), use of antisolvent treatments, gas-phase/post-treatment annealing (exposure to chemical vapors or gases), and novel physical annealing methods (rapid thermal processing, hot substrates, vacuum-assisted drying, etc.). Each approach uniquely influences the crystallization process, as overviewed below.

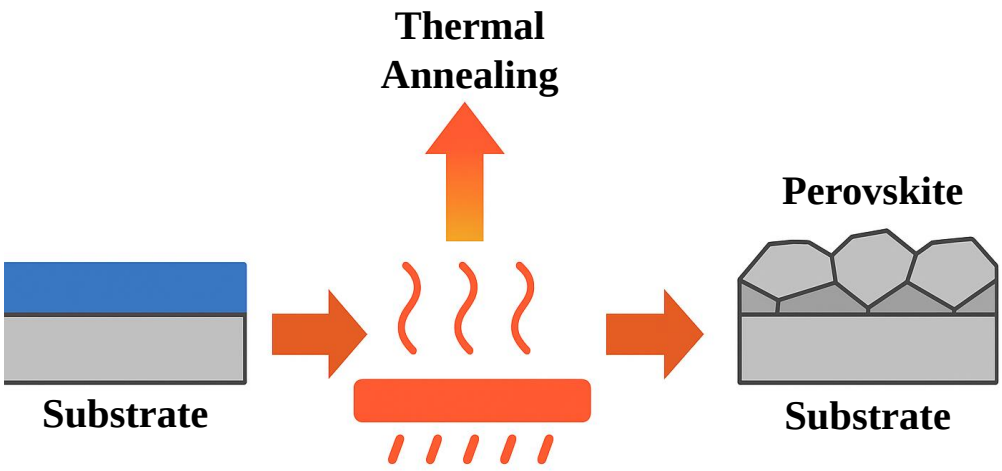

Figure 3: Schematic illustration of thermal annealing applied to perovskite films.

3.1 Thermal Annealing (Conventional)

Using only thermal annealing drives the conversion of the deposited precursor solution into a perovskite polycrystalline film. During the heating, the solvent evaporation rate and film drying dynamics strongly affect supersaturation and nucleation [7]. A moderate anneal (e.g. 100°C for 30 min) allows solvents to evaporate gradually, often leading to a moderate density of nuclei that grow and merges, yielding grain sizes of a few hundred nanometers for typical formulations. Interestingly, the thermal budget (temperature and time) can be adjusted to alter crystallization kinetics. Higher annealing temperatures for very short durations have been shown to markedly increase grain sizes. For example, Kim *et al.* demonstrated that flash-heating a wet perovskite film to 400°C for only 4 seconds caused a rapid solvent removal and supersaturation that produced grains >1 μm (versus 300 nm under standard conditions). The brief high-temperature spike promotes instantaneous nucleation across the film, followed by quick crystal growth, yielding a uniform morphology despite the large grains [37]. Such rapid thermal annealing or flash-annealing techniques can improve grain size without compromising coverage. The temperature must be precisely controlled (exceeding the decomposition threshold or applying heat for too long can degrade the perovskite). In practice, conventional thermal annealing remains the baseline for most lab-scale devices due to its simplicity and compatibility with various deposition methods. On larger substrates, thermal annealing can be accomplished with conveyor-belt furnaces or IR lamps, making it inherently scalable. The limitations of using thermal annealing are only that it may not fully eliminate defects or achieve the millimeter-scale crystalline domains as more advanced methods. Moreover, thermal annealing requires a large amount of electricity, leading to a rise in the energy recovery time for the cells.

3.2 Solvent Vapor Annealing (SVA)

Solvent annealing involves exposing the drying or fully formed perovskite film to the vapour of a solvent (or solvent mixture) to retard crystallisation and promote grain growth. The process can be achieved by either under controlled pressure or by controlled temperature. **Fig. 4** is a schematic diagram of solvent annealing under an atmospheric controlled environment. In a typical SVA process, a wet perovskite-coated substrate is placed in a closed chamber along with a small dish of solvent (such as DMF, DMSO, chlorobenzene, etc.), or the solvent is flowed over the film as a vapour. The idea, first introduced by Xiao et *al.* in 2014, is that a solvent-rich atmosphere decelerates the rate of solvent evaporation from the film during thermal annealing [11]. By maintaining a "moist" environment, the perovskite precursors stay reactive and mobile for a longer time, allowing grains to ripen than they can in dry air annealing [7]. Practically, solvent vapour softens or partially dissolves the surface of small crystallites, enabling them to merge into larger grains, an effect like Ostwald ripening but mediated by external vapour. For example, using DMF vapour during annealing was shown to increase grain sizes and form smoother $MAPbI_3$ films than dry annealing [38]. *In situ* studies confirm that SVA encourages continuous grain growth: X-ray diffraction and microscopy have revealed that extended vapour exposure causes the average crystal domain to increase as tiny grains disappear and are absorbed into larger ones [16]. One important consideration is the choice of solvent for SVA; the vapour must be able to interact with the perovskite film, typically a solvent that can partially dissolve one or more of the precursors. However, using a very strong solvent can excessively dissolve the film or cause undesirable new phases under uncontrolled vapour pressure [7]. Early SVA work with DMF or DMSO vapours requires precise control to avoid washing out the perovskite. Researchers found that using solvents with selective solubility could improve the outcome. For instance, alcohols such as ethanol or isopropanol have poor solubility for PbI_2 but can dissolve MAI; using ethanol vapour in SVA therefore primarily affects the organic MAI component, slowing the MAI/PbI_2 reaction, allowing enough time to enable defect repair without fully dissolving the film [16]. A previous study showed that isopropanol-vapour annealing led to smoother films with eliminated pinholes, presumably by dissolving excess MAI and allowing it to re-deposit in voids, while also mildly "reflowing" the perovskite grain boundaries [16]. In general, SVA tends to increase grain size (often into the micrometre range) and can improve photophysical properties by reducing trap densities. Xiao *et al.* observed an increase in device efficiency from 11% to 16% upon DMF-vapour annealing a $MAPbI_3$ film, due to enhanced crystallinity and coverage [11]. Likewise, Cao *et al.* demonstrated that incorporating a small fraction of DMSO in the precursor (which remains as a residual high-boiling solvent) and then annealing in DMF vapour led to columnar grains through solvent-mediated ripening [13]. The trade-offs of SVA include added processing time and complexity, and the need for a controlled environment to achieve reproducible results. From a scalability perspective, SVA could be implemented in a roll-to-roll coater using a solvent vapour tunnel, but maintaining

uniform vapour exposure over large areas is non-trivial. Nonetheless, solvent annealing has proven especially useful for research-scale cells to push performance via morphology improvements.

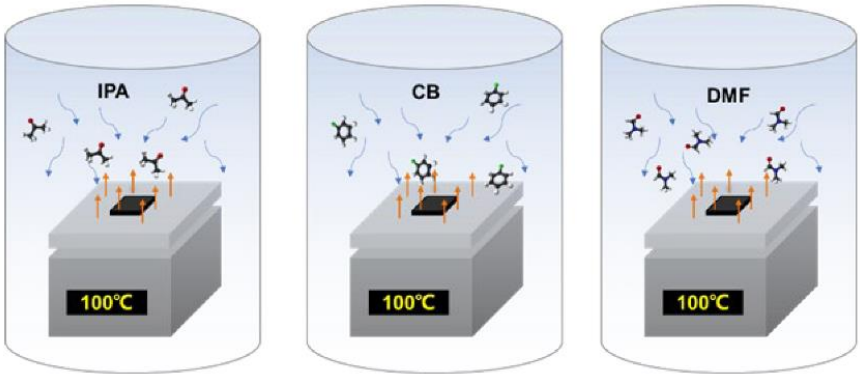

Figure 4: Schematic illustration of the atmosphere-controlled apparatus during perovskite film solvent annealing [39].

3.3 Antisolvent and Solvent Engineering during Annealing

Antisolvent treatments are closely related to solvent annealing, though typically applied during film deposition rather than post-deposition. In the one-step spin-coating method, dripping an antisolvent (e.g. chlorobenzene, toluene, diethyl ether) onto the wet perovskite film has become a standard technique to induce rapid crystallization of an intermediate phase [27, 40, 41]. This approach, often notated as anti-solvent quenching, effectively freezes the film into a solid network that can be thermally annealed to form perovskite. While not an annealing technique *per se*, antisolvent use directly impacts the subsequent annealing by dictating the starting microstructure. Fast antisolvent-induced nucleation yields many seed crystallites, so the thermal anneal that follows mainly involves grain growth from these seeds. The result is typically a pinhole-free film of relatively small grain size (hundreds of nm) but excellent uniformity. The challenge comes when scaling up: uniform dripping of antisolvent on a large substrate is impractical. To address this, scalable variants like antisolvent spraying and antisolvent bathing have been developed [42]. In one example, a mist of chlorobenzene was sprayed onto a 10 × 10 cm^2 wet film to achieve uniform nucleation; using this method, a 16 cm^2 perovskite module was made with 12.1% efficiency [43]. In another approach, slot-die coated films have been dipped briefly in an antisolvent bath to trigger crystallization uniformly across large areas [44]. These techniques blur the line between deposition and annealing but illustrate the importance of solvent engineering in controlling film formation at a large scale. Moreover, combining antisolvent steps with subsequent solvent vapor annealing can yield synergistic benefits, where the antisolvent ensures full coverage, while post-annealing in gentle solvent vapor can then enlarge the grains. Such multi-step treatments are an active area of research aimed at balancing nucleation and growth for optimal films.

3.4 Gas-Phase Post-Treatments

Beyond solvents, researchers have explored reactive gases to anneal and passivate perovskite films. A landmark example is the use of methylamine (CH_3NH_2) gas to post-treat $MAPbI_3$ films [30]. Methylamine is a small polar molecule that can reversibly intercalate into the perovskite lattice, forming a methylammonium lead iodide–methylamine adduct. Exposing a polycrystalline $MAPbI_3$ film to MA gas at room temperature solubilises the perovskite into a fluid intermediate (often visibly turning the film transparent) [45, 46]. When the MA gas is pumped out or the film is heated mildly, the perovskite recrystallises. Critically, this recrystallisation can heal cracks and gaps between grains, effectively "fusing" the polycrystalline film into a more continuous semiconductor sheet [30]. Jiang *et al.* reported that MA gas post-annealing eliminated impurities at grain boundaries and welded adjacent grains together, yielding markedly improved electronic properties [30]. Time-resolved photoluminescence showed carrier lifetimes tripled after MA gas treatment, and impedance spectra indicated a >10× increase in recombination resistance, compared to a thermally annealed control [30]. In planar PSC devices, the MA-gas-annealed films showed a 43% efficiency improvement compared to normal thermal annealing (and 20% improvement compared an equivalent solvent-vapor anneal) [30]. The mechanism is that methylamine can passivate undercoordinated Pb^{2+} or heal PbI^2-rich grain boundaries by re-dissolving and re-depositing material in

those regions [30]. Importantly, this methylamine-induced recrystallisation is reversible, allowing multiple gas exposures and removal without degrading the film, a unique advantage for defect healing. Other amines (ethylamine, etc.) have similar effects, though methylamine is most effective due to its small size and high vapour pressure. Gas-phase treatments are not limited to amines: for instance, antisolvent vapours (like diethyl ether vapour) can be flowed over a drying film to combine the effects of physical blowing and solvent annealing [47]. There are also reports of using humid air or HI/HBr vapours in post-treatment to supply missing halide and heal halide vacancy defects [33, 48]. In terms of scalability, gas-phase annealing would require a closed chamber or an in-line module where the coated substrate can be exposed uniformly to the gas. Methylamine is a hazardous gas, so any industrial adoption would need proper safety controls.

4. Mechanisms of Solvent Annealing

The SVA of perovskite films operates through a coordinated interplay of diffusion, complexation, nucleation kinetics, and ripening phenomena. Vapor Diffusion and Concentration Gradients: In an SVA environment, volatile solvent molecules permeate the perovskite film according to concentration gradients. The process can be described by Fick's second law of diffusion **Eq. (4)**, which in one dimension is [49]:

$$\frac{\partial c}{\partial t} = D\frac{\partial^2 c}{\partial t^2} \quad \textbf{(4)}$$

where: c(x, t) is the solvent concentration in the film and *D* is the solvent diffusivity. This diffusion-driven solvent transport establishes a quasi-steady solvent content throughout the film during annealing [50]. By enclosing the wet film in a solvent-rich atmosphere (e.g. a Petri dish with solvent), the evaporation rate is throttled, and a near-equilibrium vapor pressure is maintained. As a result, solvent egress is diffusion-limited rather than abrupt, yielding a gentle drying profile. According to Fick's law, a shallow concentration gradient corresponds to a slow solvent flux [7], so the film retains solvent longer time, allowing continued molecular mobility and rearrangement. This prolonged solvent presence has profound effects on crystallization: it modulates supersaturation levels over time and space in the film, directly impacting where and when nucleation occurs.

4.1 Solvent–Perovskite Complexation Equilibrium

A distinctive feature of hybrid perovskite chemistry is the ability of polar aprotic solvents (e.g. N, N-dimethylformamide, dimethyl sulfoxide) to form adduct complexes with perovskite precursors. During SVA, an equilibrium is established between free perovskite constituents and solvated intermediate phases. For example, lead halide and methylammonium halide can reversibly coordinate with DMSO vapor to form a stable intermediate (such as $(MA)2Pb_3I_8 \cdot 2DMSO$ [51]. This equilibrium can be expressed schematically:

$$\mathbf{PbI_2 + MAI + 2DMSO \rightleftharpoons (MA)_2Pb_3I_8 \,.\, 2DMSO}$$

With a formation constant favoring the complex in the presence of excess vapor. This transient adducts sequester the precursors in a partially coordinated state, effectively delaying their full conversion into the perovskite crystal lattice. In practical terms, solvent complexation raises the activation barrier for nucleation by keeping the precursors solvated (lowering the immediate supersaturation) [51]. During SVA, Le Chatelier's principle applies: the external vapor drives the equilibrium toward the complex side, sustaining a reservoir of dissolvable material that can later feed crystal growth. This mechanism is crucial in suppressing rapid nucleation. It has been observed that films annealed in solvent vapor remain in a gel-like intermediate phase for an extended period, which postpones crystallization until the solvent gradually desorbs. Such solvent-complex dynamics yield smoother conversion and often eliminate premature crystallization that would otherwise freeze in a high-defect morphology [52]. Notably, precise control of solvent partial pressure can even re-dissolve nascent crystallites: small perovskite clusters reversibly dissolve into the solvent-rich matrix (forming solvated ions/complexes) instead of irreversibly solidifying. This reversible dissolution is a cornerstone of the ripening process under SVA.

4.2 Nucleation Kinetics under SVA

Classical nucleation theory (CNT) provides a framework to understand how SVA modulates the formation of new crystalline nuclei. In solution processing, nucleation requires the system to exceed a critical supersaturation. Excess solvent vapor slows down the rate of supersaturation by keeping the film wet longer, leading to a gradual

increase in solute concentration. As a result, the critical nucleus size in solvent vapor annealing (SVA)-treated films is larger compared to rapidly dried films [53]. Since only larger nuclei are stable, smaller one's dissolve back, significantly lowering the initial nucleation density and preventing random widespread nucleation. This aligns with observations that a slow drying (or vapor-rich) environment yields fewer, larger crystalline domains as opposed to the myriad of small crystallites from fast precipitation [7]. In CNT, SVA effectively increases the nucleation activation energy by lowering supersaturation, thereby decreasing the nucleation rate. The nucleation rate J can be expressed in Arrhenius form **Eq. (5)** [22]:

$$\mathbf{J = A \exp\left(-\frac{\Delta G^*}{k_B T}\right)} \quad \textbf{(5)}$$

where: ΔG is the free energy barrier for nucleus formation. Under SVA, ΔG is higher (due to the larger critical cluster size and higher solvent-induced interfacial stability), leading to a smaller J. In practical terms, the solvent vapor *extends* the nucleation time window – crystallization onset is delayed until enough solvent has escaped to drive the system past the threshold. This delay is beneficial for film uniformity and grain size but must be balanced; if too few nuclei form initially, the film can develop large, isolated crystals or dendrites instead of a continuous layer. In optimized SVA processes, it is essential to maintain precise balance: an adequate density of nuclei forms (sometimes aided by an antisolvent or seeding step) and then SVA primarily assist the growth of these nuclei rather than initiating new ones.

4.3 Ostwald Ripening and Grain Coarsening

Once a limited number of nuclei have been established, the growth regime dominates. The continued presence of solvent vapor fosters an Ostwald ripening mechanism wherein smaller crystallites gradually dissolve and redeposit onto larger ones. Thermodynamically, this is driven by the Gibbs-Thomson relation, which quantifies the higher chemical potential (and solubility) of small particles due to their curvature. For a spherical crystal of radius r, the equilibrium concentration of dissolved species at its surface, c(r), is elevated relative to a flat interface as shown in **Eq. (6)** [54]:

$$\mathbf{c}(\boldsymbol{r}) = \boldsymbol{c}_{\infty} \exp\left(\frac{2\gamma V_m}{rRT}\right) \quad \textbf{(6)}$$

where c_∞ is the solubility for an infinitely large crystal, V_m is the molar volume, R is the gas constant, and T is the temperature. SVA supplies a quasi-liquid medium that enables this ripening: smaller grains (with higher curvature) have a greater tendency to dissolve into the residual solvent, releasing solutes that can diffuse and attach to the surfaces of larger, lower-curvature grains. In essence, the large crystals grow at the expense of the small and spontaneous coarsening process that reduces the overall surface energy of the system. The growth of an average grain radius R over time t in Ostwald ripening can often be described by a power law **Eq. (7)**:

$$\boldsymbol{R^3(t) - R^3(0) = Kt} \quad \textbf{(7)}$$

where: K is a coarsening rate constant [55]. In perovskite films undergoing SVA (or solvent-bath annealing), researchers have observed significant grain size amplification, for example, grain diameters increasing from 100 nm to 600 nm during a solvent-based anneal [50]. Such dramatic grain coarsening is a hallmark of solvent-annealed films. The residual solvent acts as a transport medium for mobile ionic species (Pb^{+2}, I^-, etc.), extending their diffusion length and thus facilitating material transfer over hundreds of nanometers [50]. Correspondingly, crystallinity improves as smaller defective grains merge into larger ones. Direct evidence of Ostwald ripening in SVA-treated perovskites is seen in the dissolution of tiny grains and the concurrent thickening of adjacent large grains during annealing. The process is essentially a self-healing of the film morphology: pinholes and grain boundary gaps are filled as material redistributes, yielding a more compact polycrystalline microstructure [56].

4.5 Integrated Effects on Morphology and Performance

Through the combined action of these mechanisms, controlled vapour diffusion, solvent complexation, nucleation regulation, and Ostwald ripening, SVA produces perovskite films with markedly enhanced morphology. Solvent-annealed films tend to exhibit larger average grain sizes, improved grain connectivity, and reduced defect densities

compared to rapidly dried films. For example, Xiao *et al.* reported that SVA increased $CH_3NH_3PbI_3$ grain size from the sub-micron scale to several microns, extending carrier diffusion lengths to >1 μm [11]. Similarly, other groups adjusted grain dimensions from 200 nm to several micrometres via solvent vapour treatments [57]. These large-grained, highly crystalline films translate to superior optoelectronic properties, reduced grain boundaries (which are recombination centres) yield longer carrier lifetimes and diffusion lengths [50]. Moreover, the gentle crystallisation afforded by SVA curbs the formation of pinholes and voids. The gradual expulsion of solvent allows the film to densify uniformly, whereas rapid solvent removal often traps voids or leaves incomplete crystallisation at grain interfaces [58]. By recrystallising small grains into larger ones, SVA effectively passivates grain boundaries and repairs defects that originate from abrupt crystallisation [56]. Crucially, each mechanism discussed synergistically reinforces the others during SVA. The slow diffusion of solvent (Fick's law) prolongs the life of solvent–perovskite complexes, which in turn delays nucleation (classical nucleation theory) and provides a medium for ripening (Ostwald via Gibbs–Thomson). Nucleation suppression means fewer grains to begin with, which makes the ripening more effective at enlarging those grains. The net outcome is a controlled crystallization pathway: nucleation is not only retarded but spatially homogenized, and subsequent crystal growth is boosted selectively for larger grains.

5. Effects of Solvent Annealing on Film Properties

Solvent annealing, exposing a freshly cast perovskite film to a controlled vapor of a solvent during thermal annealing, can profoundly influence the microstructure and performance of formamidinium-caesium (FA/Cs) lead halide perovskite films. In FA/Cs mixed-cation, typically MA-free compositions such as $FA_{1-x}Cs_xPb(I, Br)_3$, solvent annealing has been used to mediate crystallization kinetics and improve film quality. Researchers have employed solvent vapors such as N, N-dimethylformamide (DMF), dimethyl sulfoxide (DMSO), chlorobenzene (CB), and alcohols (e.g. isopropanol, IPA) to modify grain growth and defect passivation. The following section discusses how such treatments affect film morphology, the optical and electronic properties of the perovskite, and the resulting photovoltaic device performance in FA/Cs-based perovskites.

5.1 Morphological Improvements

Fig. 5 Planar SEM images of $FA_{0.85}Cs_{0.15}PbI_3$ perovskite films annealed under different atmospheres (Control, IPA, CB, DMF). The control (no solvent vapour) yields large size and uniform grains, whereas IPA and CB vapours produce smaller grains (more nucleation sites), and DMF vapour causes noticeable voids at grain boundaries (red circles) due to partial re-dissolution of the perovskite during annealing [39].

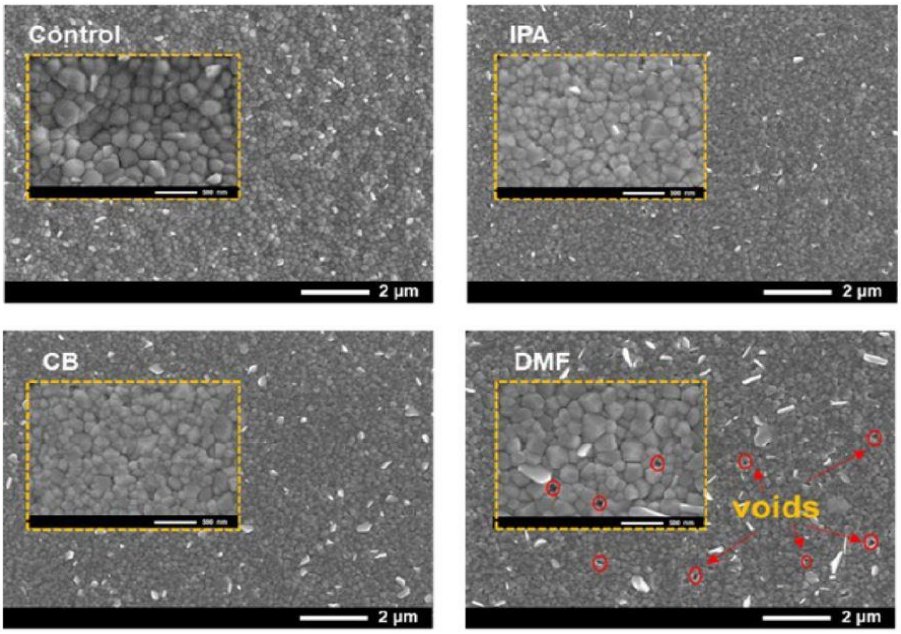

Figure 5: SEM images of $FA_{0.85}Cs_{0.15}PbI_3$ perovskite films annealed under various atmospheres (Control, IPA, CB, DMF) [39].

Solvent vapor annealing often leads to dramatic changes in film morphology. In general, introducing a small amount of a polar aprotic solvent vapor (one that can dissolve perovskite precursors) during annealing slows down crystallization and promotes Ostwald ripening of grains [59]. Smaller crystallites can partially dissolve and redeposit onto larger crystals, yielding coarsened grains and improved film coverage. For example, Peng *et al.* observed that using a controlled dose of DMF vapor during annealing grew $CH_3NH_3PbI_3$ perovskite grains from 0.33 µm (thermal annealing alone) to about 1.37 µm on average [60]. This >4× grain size increase produced a significantly more continuous, uniform FA/MA perovskite film. In FA/Cs mixed-cation compositions, solvent annealing also proves to be effective: Xiao *et al.* initially demonstrated that DMF vapor treatment could expand grain size from 260 nm to 1 µm and enhance crystallinity in a two-step FA/Cs perovskite deposition [11]. Such grain enlargement is highly beneficial, as larger grains mean fewer grain boundaries (which often harbor trap defects) and reduced perovskite/void interfacial area.

Beyond grain growth, solvent annealing can improve other morphological aspects. Optimized solvent vapor conditions tend to heal pinholes and voids in the as-cast film. A comparative study by Kim *et al.* tested different vapors (DMF, DMSO, and N-methyl-2-pyrrolidone, NMP) on FA-based perovskite films; notably, NMP vapor produced a vertically oriented, densely packed crystal morphology with virtually no pinholes [59]. The authors reported that this high-boiling solvent vapor induced a stable intermediate adduct (PbI_2-NMP complex) that regulated crystallization, resulting in a smooth, pinhole-free film. In general, repeated dissolution-recrystallisation cycles under a solvent-rich atmosphere can repair defects: the vapor softens the film and allows grains to merge, healing grain boundary gaps [61]. Indeed, annealing in DMSO or γ-butyrolactone (GBL) vapor has been shown to eliminate inter-grain voids and yield more compact perovskite layer [59].

It should be noted that the extent of improvement depends sensitively on the solvent volatility and dosage. Excessive solvent vapor or too volatile a solvent can have adverse effects on morphology. For instance, He *et al.* (2023) found that when annealing $FA_{0.85}Cs_{0.15}PbI_3$ films, the presence of a highly volatile anti-solvent vapor (IPA or CB) increased the nucleation rate significantly, which led to smaller grains than the control (no vapor). The fast evaporation of IPA/CB caused quick crystallization with many crystallites, sacrificing the large-grain morphology. On the other hand, an overly strong Lewis's base solvent such as DMF can over-solubilize the perovskite if not precisely controlled. In the same study, DMF vapor (30 µL in a sealed chamber at 100°C) partially re-dissolved the forming FA-Cs perovskite, leading to interrupted crystal growth and the appearance of voids at grain boundaries [39]. These voids (highlighted in red in **Figure 5**) create shunt pathways in devices. Thus, solvent annealing must be finely tuned; an optimal vapor exposure (e.g. a small volume of DMF for a limited time) can yield dense, large-grained films, whereas inappropriate conditions may introduce defects or inferior morphology [50]. The consensus from numerous studies is that a moderate solvent vapor treatment (using a high-boiling solvent or a minimal amount of DMF/DMSO) is most effective in achieving continuous perovskite films with enhanced crystal size and texture. **Fig. 6** presents a schematic illustration of the solvent annealing process applied to $MAPbI_3$ thin films. The figure shows the progression of DMSO vapor infiltration into the $MAPbI_3$ structure, where the solvent penetrates grain boundaries and facilitates the formation of an intermediate phase, namely MAI-PbI_2-DMSO.

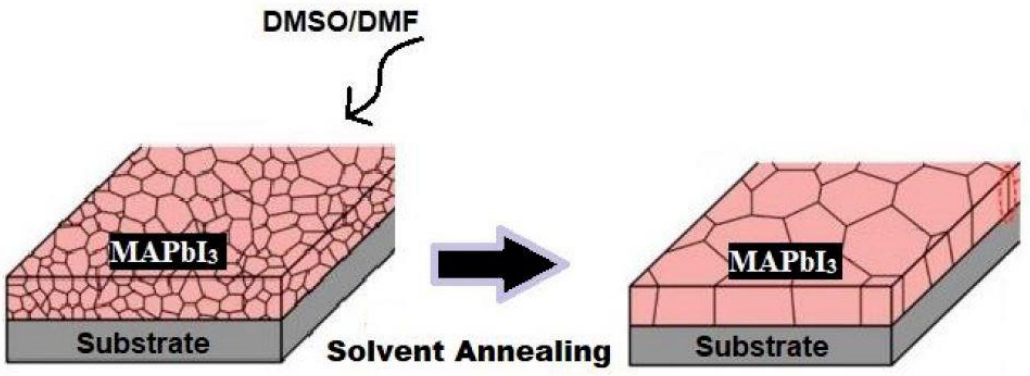

Figure 6: Schematic of the solvent annealing treatment to increase the grain size.

5.2 Optical and Electronic Properties

Solvent-annealed FA/Cs perovskite films often exhibit improved optoelectronic quality as a direct consequence of their superior morphology and crystallinity. High-quality films with enlarged grains and fewer defects tend to have lower trap densities, longer charge-carrier lifetimes, and higher photoluminescence (PL) quantum yields. For instance, the DMF-vapor-treated films in Peng *et al.*'s study showed notably stronger steady-state PL intensity and a cleaner X-ray diffraction pattern (indicating higher crystallinity) compared to thermally annealed films [60]. Likewise, solvent-vapor annealed films frequently show narrower PL emission peaks and reduced Urbach tails in absorption spectra, pointing to a reduction in disorder and defect states in the bandgap[60]. In one case, incorporating an NMP vapor step yielded a perovskite with longer performance lifetimes (by time-resolved PL) and suppressed sub-bandgap states, consistent with successful trap passivation.

Time-resolved PL measurements directly highlight the electronic gains from solvent annealing. In the $FA_{0.85}Cs_{0.15}PbI_3$ film study by He *et al.*, the control film (no vapor) exhibited an average PL decay lifetime of 21.5 ns, whereas films annealed under IPA or CB vapor had much shorter lifetimes (10-14 ns), and the DMF-vapor film was only 4.7 ns [39]. The longest lifetime in the control film was attributed to residual PbI_2 passivating traps (that condition yielded the best morphology as well). In poorly crystallized solvent-treated films, the higher density of non-radiative recombination centers (defects) led to faster PL decay. However, when solvent annealing is optimized (e.g. using the right solvent and duration), the opposite trend is observed: carrier lifetimes are prolonged due to fewer trap states and better crystal quality [59]. For example, Xiao *et al.* reported that DMF vapor processing increased the carrier recombination lifetime and mobility in FA/Cs perovskites, reflecting an overall cleaner electronic structure [11]. The reduction in grain boundaries and improved interfaces facilitates more efficient charge transport and minimizes trap-assisted recombination.

Importantly, solvent annealing typically does not alter the fundamental bandgap of the perovskite (since the chemical composition remains the same), but it can influence phase purity, which in turn affects optical behavior. FA-rich lead iodide perovskites like $FAPbI_3$ have a desired black α-phase (bandgap 1.53-1.60 eV). Some vapors can accidentally induce the yellow δ-phase $FAPbI_3$ (a wider-bandgap non-photoactive phase). He *et al.* observed that IPA vapor during annealing led to the appearance of a δ-phase peak in XRD, which corresponded with a depressed absorption in the 450-600 nm range and slightly blue-shifted emission, indicating the presence of this wider-bandgap phase. In contrast, the control and CB/DMF-treated films maintained the α-phase (same absorption edge at ~800 nm and PL peak at 795 nm). Therefore, although solvent annealing causes only slight bandgap shifts for a fixed composition, unsuitable vapor conditions can lead to phase impurities that alter the optical properties. In contrast, properly controlled solvent annealing typically results in a single-phase, high-purity perovskite with strong light absorption and high photoluminescence efficiency [39]. The trap density reduction from solvent annealing has been confirmed by techniques like space-charge limited current (SCLC) and thermal admittance spectroscopy, which show lower trap-filled limit voltages in treated films (signifying fewer deep traps) [62]. Furthermore, mixing Cs into the FA perovskite itself helps reduce trap formation, uniformly incorporating 10-15% Cs^+ in $FAPbI_3$ is reported to enhance the lattice stability and lower the intrinsic defect density [63]. Solvent annealing builds on this by improving crystallinity and removing voids, thus maximizing the optoelectronic potential of FA/Cs perovskites (long diffusion lengths, high carrier mobility, and low non-radiative recombination).

5.3 Impact on Device Performance

The ultimate motivation for solvent annealing FA/Cs perovskites is to boost photovoltaic device performance, typically quantified by the power conversion efficiency (PCE) and its sub-parameters: open-circuit voltage (Voc), short-circuit current density (Jsc), and fill factor (FF). High-quality films translate into better solar cell metrics. Many studies document significant PCE gains after introducing a solvent annealing step. For example, Kim *et al.* (with an optimized NMP vapor treatment) achieved a PCE of 15.7% in an FA-based cell, nearly doubling the efficiency from 7.8% without solvent annealing [64]. This improvement was attributed to dramatically enhanced film morphology (leading to higher photocurrent and FF). Similarly, early work by Xiao *et al.* saw PCE rise from 9.9% to 15.6% upon DMF vapor treatment in a two-step FA/Cs perovskite process [11]. These jumps in efficiency were primarily due to increased Jsc from more complete coverage and light absorption and improved Voc from reduced recombination losses.

DMF vapor treatments have yielded mixed results across studies; some report enhanced grain growth and improved crystallinity, while others note void formation and reduced device performance. Such inconsistencies are likely attributed to variations in vapor exposure, film thickness, and annealing time, underscoring the need to precisely optimize processing conditions for each specific device configuration. However, the impact of solvent annealing on performance is nuanced and depends on achieving the right balance. If the solvent vapor treatment successfully reduces traps and improves crystallinity, it can be expected to have higher Voc and higher FF thanks to suppressed non-radiative recombination [62]. Each reduction of trap density can raise Voc by tens of millivolts in these perovskites. A more uniform, pinhole-free film also enhances JSC by minimizing shunting and maximizing the photoactive area. For instance, one report on ambient-air fabrication found that adding a solvent vapor anneal (together with a small additive) yielded devices with significantly greater Jsc and FF than untreated controls, enabling PCE >20% in air-processed FA/Cs cells [65, 66]. In that case, the solvent vapor helped produce a dense morphology even under less controlled ambient conditions, bolstering all performance parameters. On the other hand, if solvent annealing is misapplied (too volatile a vapor or excess exposure), it may affect device performance. The 2023 study by He *et al.* provides a cautionary example: $FA_{0.85}Cs_{0.15}PbI_3$ solar cells that were annealed in a DMF-rich atmosphere showed a drop in PCE from 20.0% (control) to 15%, caused by the morphological defects discussed earlier. The DMF-treated devices had a markedly lower Jsc (20.8 mA/cm^2 vs 23.6 mA/cm^2 for control) and a reduced Voc (0.99 V vs 1.08 V) due to shunting and increased recombination. Interestingly, in that same work, CB-vapor-treated cells maintained a high Jsc (averaging 24.3 mA/cm^2, slightly above the control but suffered a Voc loss down to 0.99 V, likely because the CB vapor removed residual PbI_2 that was passivating the grain boundaries. This illustrates that while Jsc can improve with certain solvent vapors (due to better light harvesting from a cleaner film), Voc might decline if new trap sites or phase impurities are introduced. The fill factor similarly will drop if the film develops shunts or poor interfaces (as seen with the voids in the DMF-treated case, which drastically lowered shunt resistance and FF) [39].

Therefore, the net impact on performance is a trade-off: properly executed solvent annealing of FA/Cs perovskites yields higher efficiencies by improving all photovoltaic parameters, whereas improper treatments can compromise one or more of these parameters. In the best scenarios reported, solvent-annealed FA/Cs perovskite solar cells combine high Jsc (≥23-25 mA/cm^2), high Voc (1.1 V for bandgaps 1.6 eV), and FF in the 0.75-0.80 range, translating to PCEs in the 20-23% class for single-junction cells [62]. Moreover, beyond initial efficiency, such high-quality films often show improved operational stability, where larger grains and fewer defects slow down degradation mechanisms like moisture ingress or ion migration [67]. In sum, solvent annealing has emerged as a powerful post-deposition technique to tune FA/Cs perovskite film properties. When optimized (as many recent 2023-2024 studies demonstrate), it leads to morphologically superior films with enhanced optoelectronic properties, thereby elevating device performance. **Table 1** is a literature survey of annealing techniques in perovskite solar cells.

Table 1: Literature survey: Annealing techniques in perovskite solar cells.

Annealing Type	Solvent/Method	Reported PCE	Key Observations	Ref.
Thermal annealing (baseline)	Heat only (e.g. 100°C)	~10% (baseline)	Small grains (~0.3 μm); baseline crystallinity	[15]
DMF vapor annealing	DMF vapor (80–100 μL at ~90 °C)	≈15.1% (10.23→15.1)	Grain size ~1.3 μm (vs 0.335 μm thermally); improved film coverage	[68]
DMSO vapour annealing	DMSO vapor	13.6% (8.55→13.59)	Eliminates voids/traps, high crystallinity, and larger grains	[59]
Methanol vapour annealing (alcohol)	Methanol (MeOH) vapor	14.6% (10.2→14.6)	Highly ordered crystal growth, larger grains, ↑ and carrier lifetime	[39]
IPA: DMF mixed vapor annealing	Isopropanol/DMF (100:1 v/v) vapor	15.1% (12.2→15.1)	Dense, compact films; reduced defects; improved absorption	[69]
DMF + H_2O vapor annealing	DMF vapor + ~2% H_2O	16.8% (9.68→16.83)	Large grains (~2 μm); pinhole-free, no horizontal boundaries	[70]

DMSO + H_2O vapor annealing	DMSO vapor + H_2O (75:25 v/v)	19.5% (16.94→19.51)	Preferred grain orientation; grains ~300–900 nm vs 200–400 nm; higher crystallinity	[66]
DMSO: CB mixed vapour annealing	DMSO: chlorobenzene (1:2) vapour	18.5% (15.69→18.51)	Grain area ↑ from 0.059→0.67 μm²; fused grains; enhanced interface extraction	[71]
GBL vapor annealing	Gamma-butyrolactone (GBL) vapour	16.6% (13.05→16.58)	Grain size ↑ (193→253 nm); improved crystallinity	[72]
NMP vapor annealing	N-Methyl-2-pyrrolidone (NMP) vapour	15.7% (7.85→15.71)	Pinhole-free morphology; longer carrier lifetime	[59]
Flash (IR) annealing	Rapid IR pulse (≈0.64 s, FIRA)	18.5% (champion)	Ultra-fast (<1 s) processing; high crystallinity; stable (90% PCE after 1500 h)	[17]
Methylamine gas annealing	Methylamine (MA^0) vapor	21.4% (stabilised)	Millimetre-scale single crystals; low trap density; >80% PCE retention after 200 h	[17]
Vacuum + thermal annealing (VTA)	Vacuum + heat (post-antisolvent)	27.7% avg (32.0% peak)	Compact, dense films; suppressed trap states; record efficiency (indoor, carbon)	[73]

6. Scalability Challenges

Scaling solvent-vapor annealing from small-area laboratory cells to large-area FA/Cs perovskite modules introduces multiple technical hurdles. First, achieving a uniform solvent vapor atmosphere over large substrates is nontrivial. In lab setups, solvent annealing is often done in sealed Petri dishes or small chambers; in production, however, ensuring even vapor concentration and temperature across meter-scale rolls or panels is difficult. Non-uniform vapor can create spatial gradients in crystallization kinetics and grain growth, leading to uneven film morphology and performance. Roll-to-roll (R2R) processing demands uniform, large-area deposition to be effective [74]. In practice, designing large chambers or conveyor ovens with precise flow and saturation control (for example, via mass flow controllers or baffles) is required, but any slight temperature or flow asymmetry can cause inhomogeneity. Moreover, solvent vapors tend to escape or condense unevenly, so maintaining a stable supersaturated environment is challenging [75]. For example, uncontrolled DMF vaporization has been shown to damage films (causing pinholes) if not carefully regulated [16].

6.1 Solvent Atmosphere Control

Large-scale systems would require continuous monitoring and regulation of vapor pressure and temperature, analogous to CVD systems. Even so, differences in local saturation could yield nonuniform crystallization. Studies have shown that modest changes in solvent environment (e.g. polarity or partial pressure) significantly affect film quality.

To date, only a few experimental studies have demonstrated semi-scalable solvent annealing setups. For instance, vapor exposure chambers have been adapted for 25-40 cm^2 devices, but no consistent roll-to-roll demonstrations have been published. Realizing industrial success will require robust vapor control systems, inline monitoring, and integration with fast-moving production lines.

6.2 Analogous Methods

Some approaches avoid this issue altogether: hybrid CVD methods bypass solvents because they are challenging to control in industrial, large-scale fabrication [76]. This highlights that any solution-based process (including solvent annealing) will need very tight process control to match the uniformity of vacuum methods.

Second, environmental and safety control is a major concern. Typical perovskite solvents (DMF, DMSO, NMP, etc.) are toxic and flammable. Handling large volumes of these vapors in production requires rigorous ventilation, solvent recovery, and explosion-proof equipment. For example, even high-boiling additives like DMSO must be

carefully confined, since escaped vapors can contaminate the line and pose health hazards. Some R2R approaches have substituted more benign solvents (e.g. tert-butanol as an "eco-friendly" antisolvent [74]), but for solvent annealing, the alternatives are less explored. In addition, perovskite fabrication is usually done in inert/dry environments to exclude moisture, so adding a solvent vapor step complicates the glove-box or dry-room requirements. Process streams must scrub or recycle the solvent vapor by condensation, which increases the operation cost. Overall, the need for strict environmental control, such as low humidity, oxygen, and solvent emission limits, significantly complicates throughput.

Third, throughput and compatibility with high-speed manufacturing are challenging. Solvent annealing is typically a time-consuming step: film exposure duration in vapor ranged from minutes to tens of minutes to allow Ostwald ripening and crystal growth. In contrast, industrial R2R lines demand very short dwell times (often seconds) per section to achieve tens of meters/minute speeds. Integrating a slow vapor-anneal step would bottleneck throughput. Even if a tunnel oven is used, it would need extremely long residence (tens of meters of conveyor) or multiple parallel zones to handle vapor saturation, making the line unwieldy. By comparison, most experimental R2R demonstrations rely on rapid antisolvent dipping or flash-curing techniques precisely because they fit high throughput. In practice, engineers must balance the improved film quality from solvent annealing against the increased cycle time; too slow a process negates the economic benefits of R2R manufacturing.

Finally, reproducibility across modules becomes more difficult at a large scale. Small-area studies have shown good repeatability: for example, Yu *et al.* achieved very consistent PCEs across 40 devices using room-temperature vapor annealing [77]. However, it is hard to achieve uniformity over tens or hundreds of cm^2. Film thickness variations, edge effects (solvent escaping at film borders), and non-ideal module geometries all contribute to variability. Small fluctuations in solvent composition or temperature between batches can lead to noticeable shifts in crystallization behavior. In an industrial setting, even slight conveyor speed variations or ambient changes (e.g. humidity spikes) could induce differences from one module to the next. Ensuring that each square meter receives the same vapor exposure, and thus the same crystal size and defect passivation, requires stringent process control and possibly inline metrology; without such controls, module-to-module reproducibility is inconsistent, leading to reduced yield.

7. Environmental and Toxicity Considerations

A major limitation of solvent annealing is the reliance on toxic solvents such as DMF and DMSO, which pose health and environmental risks. These solvents require closed-loop systems and solvent recovery infrastructure for safe and large-scale use. Alternative low-toxicity solvents, such as alcohol or n-butanol, offer safer options but require further optimization for better performance.

8. Future Directions

8.1. Integration with Perovskite-Silicon Tandems

Perovskite/silicon tandem cells are a key target, but integrating solvent annealing into tandem fabrication poses new demands. In tandem devices, the perovskite layer often must conform to a textured Si bottom cell; smooth, conformal growth is required to avoid voids. Vacuum-deposited perovskites naturally coat textured surfaces [76]; future work is suggested to adapt solvent annealing for such topography. For example, vapor annealing could help flow the perovskite into facets and heal roughness. Recent work has already shown that careful solvent selection enables high-efficiency tandem films. Zheng *et al.* demonstrated that using low-polarity n-butanol vapor during deposition in air greatly suppressed moisture damage on textured silicon, yielding 29.4% certified tandem efficiency on 16 cm^2 substrates [78]. This suggests that solvent engineering (choosing vapors with moderate volatility and polarity) can both protect the perovskite in ambient conditions and improve film uniformity for large-area tandem cells [78]. Going forward, hybrid annealing approaches (combining vapor exposure with low-temperature heat or light-curing) may be developed to produce uniform perovskite layers atop silicon without damaging the bottom cell.

8.2 Solvent System Innovations

Continued innovation in solvent formulations is a promising future direction. Instead of classical DMF/DMSO, researchers are exploring mixed or alternative solvents for annealing. For instance, replacing DMF with alcohol

vapors (ethanol, isopropanol, etc.) has been shown to selectively dissolve FAI over PbI_2, filling pinholes and passivating defects. Recent studies suggested that by tuning solvent polarity and boiling point, the crystallization rate can be controlled and avoid film damage. Moreover, bio-based or low-toxicity solvents (e.g. n-butanol, tert-butyl alcohol) are being tested because of their wide processing windows and safer handling [78]. Future solvent mixtures might incorporate additives that remain in the film as passivators or employ solvent-vapor mixtures (as in "mixed-vapor annealing") to achieve a balance between drying speed and crystal growth. Such innovations could expand the processing window, making the annealing step more applicable and suitable for large-scale production.

8.3 Automated Vapor Annealing in Manufacturing

Automation of the solvent annealing step will be critical for industrial adoption. This will likely involve in-line equipment that delivers controlled solvent vapor to moving substrates. One vision is a segmented R2R chamber: for example, a series of enclosed ovens into which solvent is injected at controlled rates, with sensors monitoring vapor concentration and film temperature in real time. Feedback loops (PID controllers) could adjust solvent flow to maintain uniform conditions as web speed changes. Robotic systems could automate the loading and unloading of sheets during batch processing, efficiently moving modules into and out of vapor chambers. Meanwhile, machine-learning algorithms could dynamically optimize annealing profiles in real time by analyzing film thickness data or optical signals. While few such systems exist today, experimental R2R lines (e.g. gravure printing with antisolvent bathing) demonstrate that partial automation is feasible [78]. Future work will adapt these concepts specifically for vapor annealing, perhaps by combining thermal flash-curing (for speed) with a brief, automated vapor treatment (for quality).

8.4 Long-Term Stability Strategies

Despite that, solvent annealing has shown promising performance improvements, but research gaps remain unsolved. These include limited understanding of vapor-perovskite interactions at different scales, inconsistent data on long-term stability under ambient conditions, and a lack of in situ studies to monitor crystallization dynamics. Moreover, the absence of standardized protocols and limited reproducibility in large-area modules hinders industrial deployment.

Finally, solvent annealing must be combined with broader stability improvements. One trend is compositional engineering: incorporating inorganic cations (Cs, Rb, K) into the FA-PbI_3 lattice markedly improves thermal and moisture stability. Indeed, RSC reports note that triple-cation (Cs/FA/MA) films now show 1000 h endurance under damp-heat tests (85 % RH, 25°C) on 25 cm^2 modules [76]. Future solvent annealing protocols could exploit this by co-annealing alkali-metal iodide vapors (e.g. CsI) to simultaneously crystallize and dope the film. Surface/passivation layers are another key strategy. Research on 2D/3D hybrid perovskites indicates that thin 2D cap layers or mixed-dimensional salts at grain boundaries dramatically suppress moisture ingress [79]. Integrating such passivation during solvent annealing (for example, by using vaporized 2D organic salts) is a promising direction. Encapsulation complements all of this; advanced barrier coatings will be needed to lock in any moisture-resilient film.

9. Conclusions

This review highlights that solvent-assisted annealing fundamentally alters perovskite crystal growth by modulating the evaporation kinetics of precursor solvents. Introducing a carefully chosen solvent vapor during thermal annealing prolongs the dissolution–recrystallisation process. The extended dwell time of the solvent in the film drives Ostwald ripening: small nuclei dissolve and redeposit on larger grains, resulting in a few large (>1 μm) grains instead of many tiny ones. Prolonged annealing in residual solvent markedly increases grain size via this ripening mechanism. Crucially, the choice of solvent or vapor is tailored: aggressive solvents like DMSO or DMF must be regulated (to prevent film damage), whereas vapors such as alcohols (e.g., ethanol, isopropanol) selectively remove methylammonium iodide and passivate surface defects during an annealing.

These microstructural improvements from solvent annealing have significant performance impacts. Larger grains and healed grain boundaries reduce nonradiative recombination and extend carrier diffusion lengths, directly benefiting device metrics. Solvent-annealed films have demonstrated high carrier diffusion lengths and strong

performance even for thick layers. Dual-vapor treatments have pushed laboratory efficiencies further, enabling nearly single-crystalline microstructures and significantly reduced trap densities. Across multiple studies, solvent-annealed devices also show enhanced stability, likely because better crystallinity and defect passivation inhibit moisture ingress and phase degradation. Thus, solvent annealing not only boosts initial power conversion efficiency, but also improves device durability.

Looking toward scalability and industrial implementation, solvent-annealing presents both opportunities and challenges. Some treatments are already compatible with ambient, large-area processing, producing films with micrometer-scale grains and full surface coverage. This paves the way for integration with scalable methods like blade or slot-die coating using controlled vapor zones. However, challenges remain in uniformly controlling vapor composition over large substrates and addressing solvent toxicity. Future research should focus on mechanistic studies, solvent innovation, process integration, and long-term stability validation to fully realize the potential of solvent annealing in commercial perovskite solar cells.

Conflict of Interest

The authors declare that they have no conflict of interest.

References

[1] C. Yang, W. Hu, J. Liu, C. Han, Q. Gao, A. Mei, *et al.*, "Achievements, challenges, and future prospects for industrialization of perovskite solar cells," *Light Sci. Appl.*, vol. 13, no. 1, p. 227, 2024, doi: 10.1038/s41377-024-01461-x.

[2] K. T. Tanko, Z. Tian, S. Raga, H. Xie, E. A. Katz, and M. Lira-Cantu, "Stability and reliability of perovskite photovoltaics: Are we there yet?," *MRS Bull.*, vol. 50, no. 4, pp. 512–525, 2025, doi: 10.1557/s43577-025-00863-5.

[3] A. Kojima, K. Teshima, Y. Shirai, and T. Miyasaka, "Organometal Halide Perovskites as Visible-Light Sensitizers for Photovoltaic Cells," *J. Am. Chem. Soc.*, vol. 131, no. 17, pp. 6050–6051, May 2009, doi: 10.1021/ja809598r.

[4] NREL, "NREL," *National Renewable Energy Labratories*, 2021. https://www.nrel.gov/

[5] Z. Li, T. R. Klein, D. H. Kim, M. Yang, J. J. Berry, M. F. A. M. Van Hest, K. Zhu., "Scalable fabrication of perovskite solar cells," *Nat. Rev. Mater.*, vol. 3, no. 4, p. 18017, 2018, doi: 10.1038/natrevmats.2018.17.

[6] H. J. Snaith, "Perovskites: The Emergence of a New Era for Low-Cost, High-Efficiency Solar Cells," *J. Phys. Chem. Lett.*, vol. 4, no. 21, pp. 3623–3630, Nov. 2013, doi: 10.1021/jz4020162.

[7] M. Abbas, L. Zeng, F. Guo, M. Rauf, X.-C. Yuan, and B. Cai, "A Critical Review on Crystal Growth Techniques for Scalable Deposition of Photovoltaic Perovskite Thin Films.," *Mater. (Basel, Switzerland)*, vol. 13, no. 21, Oct. 2020, doi: 10.3390/ma13214851.

[8] N. J. Jeon, J. H. Noh, Y. C. Kim, W. S. Yang, S. Ryu, and S. Il Seok, "Solvent engineering for high-performance inorganic–organic hybrid perovskite solar cells," *Nat. Mater.*, vol. 13, no. 9, pp. 897–903, 2014, doi: 10.1038/nmat4014.

[9] J. Y. Kim, J.-W. Lee, H. S. Jung, H. Shin, and N.-G. Park, "High-Efficiency Perovskite Solar Cells," *Chem. Rev.*, vol. 120, no. 15, pp. 7867–7918, Aug. 2020, doi: 10.1021/acs.chemrev.0c00107.

[10] M. R. Leyden, L. K. Ono, S. R. Raga, Y. Kato, S. Wang, and Y. Qi, "High performance perovskite solar cells by hybrid chemical vapor deposition," *J. Mater. Chem. A*, vol. 2, no. 44, pp. 18742–18745, 2014, doi: 10.1039/C4TA04385E.

[11] Z. Xiao, Q. Dong, C. Bi, Y. Shao, Y. Yuan, and J. Huang, "Solvent Annealing of Perovskite-Induced Crystal Growth for Photovoltaic-Device Efficiency Enhancement," *Adv. Mater.*, vol. 26, no. 37, pp. 6503–6509, Oct. 2014, doi: https://doi.org/10.1002/adma.201401685.

[12] G. Liu, X. Xie, Z. Liu, G. Cheng, and E.-C. Lee, "Alcohol based vapor annealing of a poly(3,4-ethylenedioxythiophene):poly(styrenesulfonate) layer for performance improvement of inverted perovskite solar cells," *Nanoscale*, vol. 10, no. 23, pp. 11043–11051, 2018, doi: 10.1039/C8NR02146E.

[13] X. Cao *et al.*, "Fabrication of Perovskite Films with Large Columnar Grains via Solvent-Mediated Ostwald Ripening for Efficient Inverted Perovskite Solar Cells," *ACS Appl. Energy Mater.*, vol. 1, no. 2, pp. 868–875, Feb. 2018, doi: 10.1021/acsaem.7b00300.

[14] Y. Zheng, S. Li, D. Zheng, and J. Yu, "Effects of different polar solvents for solvent vapor annealing treatment on the performance of polymer solar cells," *Org. Electron.*, vol. 15, no. 11, pp. 2647–2653, 2014, doi: https://doi.org/10.1016/j.orgel.2014.07.026.

[15] L. Wang, G. Liu, X. Xi, G. Yang, L. Hu, B. Zhu, *et al.*, "Annealing Engineering in the Growth of Perovskite Grains," *Crystals*, vol. 12, no. 7. 2022. doi: 10.3390/cryst12070894.

[16] C. Liu, K. Wang, C. Yi, X. Shi, A. W. Smith, X. Gong, A. J. Heeger. "Efficient Perovskite Hybrid Photovoltaics via Alcohol-Vapor Annealing Treatment," *Adv. Funct. Mater.*, vol. 26, no. 1, pp. 101–110, Jan. 2016, doi: https://doi.org/10.1002/adfm.201504041.

[17] Y. Yu, C. Wang, C. R. Grice, N. Shrestha, D. Zhao, W. Liao, *et al.*, "Synergistic Effects of Lead Thiocyanate Additive

and Solvent Annealing on the Performance of Wide-Bandgap Perovskite Solar Cells," *ACS Energy Lett.*, vol. 2, no. 5, pp. 1177–1182, May 2017, doi: 10.1021/acsenergylett.7b00278.

[18] Z. Wang, X. Duan, J. Zhang, W. Yuan, D. Qu, Y. Chen, *et al.*, "Manipulating the crystallization kinetics of halide perovskites for large-area solar modules," *Commun. Mater.*, vol. 5, no. 1, p. 131, 2024, doi: 10.1038/s43246-024-00566-5.

[19] X. Tang, Z. Wang, D. Wu, Z. Wu, Z. Ren, R. Li, *et al.*, "In Situ Growth Mechanism for High-Quality Hybrid Perovskite Single-Crystal Thin Films with High Area to Thickness Ratio: Looking for the Sweet Spot," *Adv. Sci.*, vol. 9, no. 13, p. 2104788, May 2022, doi: https://doi.org/10.1002/advs.202104788.

[20] Z. Wang, C. Shan, C. Liu, X. Tang, D. Luo, H. Tang, *et al.*, "In situ growth of perovskite single-crystal thin films with low trap density," *Cell Reports Phys. Sci.*, vol. 4, no. 4, Apr. 2023, doi: 10.1016/j.xcrp.2023.101363.

[21] C. Liu, Y.-B. Cheng, and Z. Ge, "Understanding of perovskite crystal growth and film formation in scalable deposition processes," *Chem. Soc. Rev.*, vol. 49, no. 6, pp. 1653–1687, 2020, doi: 10.1039/C9CS00711C.

[22] D. Zheng, F. Raffin, P. Volovitch, and T. Pauporté, "Control of perovskite film crystallization and growth direction to target homogeneous monolithic structures," *Nat. Commun.*, vol. 13, no. 1, p. 6655, 2022, doi: 10.1038/s41467-022-34332-3.

[23] C. Wu, K. Wang, J. Li, Z. Liang, J. Li, W. Li, *et al.*, "Volatile solution: the way toward scalable fabrication of perovskite solar cells?," *Matter*, vol. 4, no. 3, pp. 775–793, 2021, doi: 10.1016/j.matt.2020.12.025.

[24] N. Ahn, D.-Y. Son, I.-H. Jang, S. M. Kang, M. Choi, and N.-G. Park, "Highly Reproducible Perovskite Solar Cells with Average Efficiency of 18.3% and Best Efficiency of 19.7% Fabricated via Lewis Base Adduct of Lead(II) Iodide," *J. Am. Chem. Soc.*, vol. 137, no. 27, pp. 8696–8699, Jul. 2015, doi: 10.1021/jacs.5b04930.

[25] Y. Guo, K. Shoyama, W. Sato, Y. Matsuo, K. Inoue, K. Harano, *et al.*, "Chemical Pathways Connecting Lead(II) Iodide and Perovskite via Polymeric Plumbate(II) Fiber," *J. Am. Chem. Soc.*, vol. 137, no. 50, pp. 15907–15914, Dec. 2015, doi: 10.1021/jacs.5b10599.

[26] W. Xiang, J. Zhang, S. (Frank) Liu, S. Albrecht, A. Hagfeldt, and Z. Wang, "Intermediate phase engineering of halide perovskites for photovoltaics," *Joule*, vol. 6, no. 2, pp. 315–339, 2022, doi: 10.1016/j.joule.2021.11.013.

[27] M. Kim, G. H. Kim, T. K. Lee, I. W. Choi, H. W. Choi, Y. Jo, *et al.*, "Methylammonium Chloride Induces Intermediate Phase Stabilization for Efficient Perovskite Solar Cells," *Joule*, vol. 3, no. 9, pp. 2179–2192, Sep. 2019, doi: 10.1016/j.joule.2019.06.014.

[28] W. Zuo, M. M. Byranvand, T. Kodalle, M. Zohdi, J. Lim, B. Carlsen, *et al.*, "Coordination Chemistry as a Universal Strategy for a Controlled Perovskite Crystallization," *Adv. Mater.*, vol. 35, no. 39, p. 2302889, Sep. 2023, doi: https://doi.org/10.1002/adma.202302889.

[29] S. Bera, A. Saha, S. Mondal, A. Biswas, S. Mallick, R. Chatterjee, S. Roy, "Review of defect engineering in perovskites for photovoltaic application," *Mater. Adv.*, vol. 3, no. 13, pp. 5234–5247, 2022, doi: 10.1039/D2MA00194B.

[30] Y. Jiang, E. J. Juarez-Perez, Q. Ge, S. Wang, M. R. Leyden, L. K. Ono, *et al.*, "Post-annealing of MAPbI3 perovskite films with methylamine for efficient perovskite solar cells," *Mater. Horizons*, vol. 3, no. 6, pp. 548–555, 2016, doi: 10.1039/C6MH00160B.

[31] W. Nie, H. Tsai, R. Asadpour, J. C. Blancon, A. J. Neukirch, G. Gupta, *et al.*, "High-efficiency solution-processed perovskite solar cells with millimeter-scale grains," *Science (80-.).*, vol. 347, no. 6221, pp. 522–525, Jan. 2015, doi: 10.1126/science.aaa0472.

[32] J. Zhang, S. Tang, M. Zhu, Z. Li, Z. Cheng, S. Xiang, Z. Zhang, "The Role of Grain Boundaries in Organic–Inorganic Hybrid Perovskite Solar Cells and its Current Enhancement Strategies: A Review," *ENERGY Environ. Mater.*, vol. 7, no. 4, p. e12696, Jul. 2024, doi: https://doi.org/10.1002/eem2.12696.

[33] W. Kaiser, K. Hussain, A. Singh, A. A. Alothman, D. Meggiolaro, A. Gagliardi, *et al.*, "Defect formation and healing at grain boundaries in lead-halide perovskites," *J. Mater. Chem. A*, vol. 10, no. 46, pp. 24854–24865, 2022, doi: 10.1039/D2TA06336K.

[34] M. Saliba, T. Matsui, J. Y. Seo, K. Domanski, J. P. Correa-Baena, M. K. Nazeeruddin *et al.*, "Cesium-containing triple cation perovskite solar cells: improved stability, reproducibility and high efficiency," *Energy Environ. Sci.*, vol. 9, no. 6, pp. 1989–1997, 2016, doi: 10.1039/C5EE03874J.

[35] M. M. Byranvand, C. Otero-Martínez, J. Ye, W. Zuo, L. Manna, M. Saliba, *et al.*, "Recent Progress in Mixed A-Site Cation Halide Perovskite Thin-Films and Nanocrystals for Solar Cells and Light-Emitting Diodes," *Adv. Opt. Mater.*, vol. 10, no. 14, p. 2200423, Jul. 2022, doi: https://doi.org/10.1002/adom.202200423.

[36] S. Takahashi, S. Uchida, and H. Segawa, "Effect of Chloride Incorporation on the Intermediate Phase and Film Morphology of Methylammonium Lead Halide Perovskites," *ACS Omega*, vol. 8, no. 45, pp. 42711–42721, Nov. 2023, doi: 10.1021/acsomega.3c05463.

[37] M. Kim, G. H. Kim, K. S. Oh, Y. Jo, H. Yoon, K. H. Kim, *et al.*, "High-Temperature–Short-Time Annealing Process for High-Performance Large-Area Perovskite Solar Cells," *ACS Nano*, vol. 11, no. 6, pp. 6057–6064, Jun. 2017, doi: 10.1021/acsnano.7b02015.

[38] S. Xiao, Y. Bai, X. Meng, T. Zhang, H. Chen, X. Zheng, *et al.*, "Unveiling a Key Intermediate in Solvent Vapor

Postannealing to Enlarge Crystalline Domains of Organometal Halide Perovskite Films," *Adv. Funct. Mater.*, vol. 27, no. 12, p. 1604944, Mar. 2017, doi: https://doi.org/10.1002/adfm.201604944.

[39] M. He, S. Chen, T. Wang, G. Xu, N. Liu, and F. Xu, "Effects of Solvent Vapor Atmosphere on Photovoltaic Performance of Perovskite Solar Cells," *Crystals*, vol. 13, no. 4. 2023. doi: 10.3390/cryst13040549.

[40] S. Yang, S. Chen, E. Mosconi, Y. Fang, X. Xiao, C. Wang, *et al.*, "Stabilizing halide perovskite surfaces for solar cell operation with wide-bandgap lead oxysalts," *Science (80-.).*, vol. 365, no. 6452, pp. 473–478, Aug. 2019, doi: 10.1126/science.aax3294.

[41] E. H. Jung, N. J. Jeon, E. Y. Park, C. S. Moon, T. J. Shin, T. Y. Yang, *et al.*, "Efficient, stable and scalable perovskite solar cells using poly(3-hexylthiophene)," *Nature*, vol. 567, no. 7749, pp. 511–515, 2019, doi: 10.1038/s41586-019-1036-3.

[42] Y. Zhou, M. Yang, W. Wu, A. L. Vasiliev, K. Zhu, and N. P. Padture, "Room-temperature crystallization of hybrid-perovskite thin films via solvent–solvent extraction for high-performance solar cells," *J. Mater. Chem. A*, vol. 3, no. 15, pp. 8178–8184, 2015, doi: 10.1039/C5TA00477B.

[43] J. Kim, J. S. Yun, Y. Cho, D. S. Lee, B. Wilkinson, A. M. Soufiani, *et al.*, "Overcoming the Challenges of Large-Area High-Efficiency Perovskite Solar Cells," *ACS Energy Lett.*, vol. 2, no. 9, pp. 1978–1984, Sep. 2017, doi: 10.1021/acsenergylett.7b00573.

[44] A. Sandström, H. F. Dam, F. C. Krebs, and L. Edman, "Ambient fabrication of flexible and large-area organic light-emitting devices using slot-die coating," *Nat. Commun.*, vol. 3, no. 1, p. 1002, 2012, doi: 10.1038/ncomms2002.

[45] D. Ma, J. X. Zhong, X. Zhuang, C. Xu, W. Wang, H. Wang, *et al.*, "Perovskite grain fusion strategy via controlled methylamine gas release for efficient and stable formamide-based perovskite solar cells," *Chem. Eng. J.*, vol. 475, p. 146267, 2023, doi: https://doi.org/10.1016/j.cej.2023.146267.

[46] Z. Zhou, Z. Wang, Y. Zhou, S. Pang, D. Wang, H Xu, *et al.*, "Methylamine-Gas-Induced Defect-Healing Behavior of $CH_3NH_3PbI_3$ Thin Films for Perovskite Solar Cells.," *Angew. Chemie*, vol. 54 33, pp. 9705–9709, 2015,. Available: https://api.semanticscholar.org/CorpusID:25978317

[47] F. Huang, Y. Dkhissi, W. Huang, M. Xiao, I. Benesperi, S. Rubanov, *et al.*, "Gas-assisted preparation of lead iodide perovskite films consisting of a monolayer of single crystalline grains for high efficiency planar solar cells," *Nano Energy*, vol. 10, pp. 10–18, 2014, doi: https://doi.org/10.1016/j.nanoen.2014.08.015.

[48] Z. Guo, M. Yuan, G. Chen, F. Liu, R. Lu, and W.-J. Yin, "Understanding Defects in Perovskite Solar Cells through Computation: Current Knowledge and Future Challenge," *Adv. Sci.*, vol. 11, no. 20, p. 2305799, May 2024, doi: https://doi.org/10.1002/advs.202305799.

[49] A. Hinderhofer and F. Schreiber, "Organic-Organic Heterostructures: Concepts and Applications," *Chemphyschem*, vol. 13, pp. 628–643, Feb. 2012, doi: 10.1002/cphc.201100737.

[50] R. Meng, C. Li, L. Yang, Z. Li, Z. Wan, J. Shi, Z. Li, "Solvent bath annealing-induced liquid phase Ostwald ripening enabling efficient and stable perovskite solar cells," *J. Mater. Chem. A*, vol. 11, no. 9, pp. 4780–4788, 2023, doi: 10.1039/D2TA09795H.

[51] J. Cao, X. Jing, J. Yan, C. Hu, R. Chen, J. Yin, *et al.*, "Identifying the Molecular Structures of Intermediates for Optimizing the Fabrication of High-Quality Perovskite Films.," *J. Am. Chem. Soc.*, vol. 138, no. 31, pp. 9919–9926, Aug. 2016, doi: 10.1021/jacs.6b04924.

[52] M. Yang, T. Zhang, P. Schulz, Z. Li, G. Li, D. H. Kim, *et al.*, "Facile fabrication of large-grain $CH_3NH_3PbI_3$−xBrx films for high-efficiency solar cells via CH_3NH_3Br-selective Ostwald ripening," *Nat. Commun.*, vol. 7, no. 1, p. 12305, 2016, doi: 10.1038/ncomms12305.

[53] N. T. K. Thanh, N. Maclean, and S. Mahiddine, "Mechanisms of Nucleation and Growth of Nanoparticles in Solution," *Chem. Rev.*, vol. 114, no. 15, pp. 7610–7630, Aug. 2014, doi: 10.1021/cr400544s.

[54] J. Moon, S. Kwon, M. Alahbakhshi, Y. Lee, K. Cho, A. Zakhidov, *et al.*, "Surface Energy-Driven Preferential Grain Growth of Metal Halide Perovskites: Effects of Nanoimprint Lithography Beyond Direct Patterning," *ACS Appl. Mater. Interfaces*, vol. 13, Jan. 2021, doi: 10.1021/acsami.0c17655.

[55] J. Xiang, C. Han, Y. Cheng, Q. Gao, W. Hu, Y. Zhou, *et al.*, "Recent Progress and Advances of Perovskite Crystallization in Carbon-Based Printable Mesoscopic Solar Cells," *Adv. Mater.*, vol. 37, no. 9, p. 2415405, Mar. 2025, doi: https://doi.org/10.1002/adma.202415405.

[56] J. Höcker, D. Kiermasch, P. Rieder, K. Tvingstedt, A. Baumann, and V. Dyakonov, "Efficient Solution Processed $CH_3NH_3PbI_3$ Perovskite Solar Cells with PolyTPD Hole Transport Layer," vol. 74, no. 8, pp. 665–672, 2019, doi: doi:10.1515/zna-2019-0127.

[57] Y. Zhong, D. Seeberger, E. M. Herzig, A. Köhler, F. Panzer, C. Li, S. Huettner, "The Impact of Solvent Vapor on the Film Morphology and Crystallization Kinetics of Lead Halide Perovskites during Annealing," *ACS Appl. Mater. Interfaces*, vol. 13, Sep. 2021, doi: 10.1021/acsami.1c09075.

[58] Y. Wang, Y. Zang, Y. Tu, W. Liu, C. Zhu, P. Zhou, *et al.*, "Efficient and Stable Inverted Perovskite Solar Cells Enabled by Inhibiting Voids via a Green Additive," *ACS Appl. Mater. Interfaces*, vol. 16, no. 47, pp. 64889–64897, Nov. 2024, doi: 10.1021/acsami.4c15597.

[59] T. Xiaohong, "Solvent Vapor Annealing of Perovskite Films for High Performance Perovskite Solar Cells: A Mini-Review," *Polym. Sci. Peer Rev. J.*, vol. 3, no. 3, pp. 1–5, 2022, doi: 10.31031/psprj.2022.03.000563.

[60] H. Peng, C. Lan, S. Chen, P. Fan, G. Liang, and H. Lan, "N,N-dimethylformamide vapor effect on microstructural and optical properties of $CH_3NH_3PbI_3$ film during solvent annealing," *Surf. Coatings Technol.*, vol. 359, pp. 162–168, 2019, doi: https://doi.org/10.1016/j.surfcoat.2018.12.069.

[61] Y. Yu, H. Du, Q. Liu, and Z. Pang, "Pressure-assisted crystallization techniques for high-performance metal halide perovskite devices," *Microstructures*, vol. 5, no. 3, p. 2025046, 2025, doi: 10.20517/microstructures.2024.144.

[62] A. Soultati, M. Tountas, K. K. Armadorou, A. R. bin M. Yusoff, M. Vasilopoulou, and M. K. Nazeeruddin, "Synthetic approaches for perovskite thin films and single-crystals," *Energy Adv.*, vol. 2, no. 8, pp. 1075–1115, 2023, doi: 10.1039/D3YA00098B.

[63] H. Chen, Y. Wang, Y. Fan, Y. Chen, Y. Miao, Z. Qin, *et al.*, "Decoupling engineering of formamidinium–cesium perovskites for efficient photovoltaics," *Natl. Sci. Rev.*, vol. 9, no. 10, p. nwac127, Oct. 2022, doi: 10.1093/nsr/nwac127.

[64] G.-H. Kim, J. Jeong, Y. J. Yoon, H. Jang, S. Kim, J. Seo, J. Y. Kim, "The optimization of intermediate semi–bonding structure using solvent vapor annealing for high performance p-i-n structure perovskite solar cells," *Org. Electron.*, vol. 65, pp. 300–304, 2019, doi: https://doi.org/10.1016/j.orgel.2018.11.034.

[65] V. S. Murugesan, M. Maitani, H. Segawa, and T. Miyasaka, "Enhancement of power conversion efficiency in cesium-based mixed cation halide perovskite solar cells by controlled perovskite crystal out of glove box using post vapor annealing," *Surfaces and Interfaces*, vol. 59, p. 105924, 2025, doi: https://doi.org/10.1016/j.surfin.2025.105924.

[66] V. O. Eze, Y. Seike, and T. Mori, "Synergistic Effect of Additive and Solvent Vapor Annealing on the Enhancement of MAPbI3 Perovskite Solar Cells Fabricated in Ambient Air," *ACS Appl. Mater. Interfaces*, vol. 12, no. 41, pp. 46837–46845, Oct. 2020, doi: 10.1021/acsami.0c08580.

[67] S. Duan, N. Tian, J. Zhang, Z. Huang, D. Yao, G. Zheng, *et al.*, "Synthesis of Stable Cs-Rich FA-Cs Perovskite Solar Cells by Assistance of a Lewis Base Additive," *ACS Appl. Energy Mater.*, vol. 7, no. 11, pp. 4826–4833, Jun. 2024, doi: 10.1021/acsaem.4c00544.

[68] R. Abdur, S. Singh, M. A. Kuddus Sheikh, M. A. A. Shaikh, M. S. Jamal, and J. Lee, "Modified post-annealing process with N, N-dimethylformamide vapor to control the growth of hybrid perovskite microstructure," *Results Mater.*, vol. 16, p. 100330, 2022, doi: https://doi.org/10.1016/j.rinma.2022.100330.

[69] X. Sun, C. Zhang, J. Chang, H. Yang, H. Xi, G. Lu, *et al.*, "Mixed-solvent-vapor annealing of perovskite for photovoltaic device efficiency enhancement," *Nano Energy*, vol. 28, pp. 417–425, 2016, doi: https://doi.org/10.1016/j.nanoen.2016.08.055.

[70] A. Yi, S. Chae, H. Lee, and H. J. Kim, "The synergistic effect of cooperating solvent vapor annealing for high-efficiency planar inverted perovskite solar cells," *J. Mater. Chem. A*, vol. 7, no. 48, pp. 27267–27277, 2019, doi: 10.1039/C9TA08791E.

[71] B. Li, T. Jiu, C. Kuang, S. Ma, Q. Chen, X. Li, J. Fang, "Chlorobenzene vapor assistant annealing method for fabricating high quality perovskite films," *Org. Electron.*, vol. 34, pp. 97–103, 2016, doi: https://doi.org/10.1016/j.orgel.2016.04.024.

[72] J. Luo, R. Z. Qiu, Z. S. Yang, Y. X. Wang, and Q. F. Zhang, "Mechanism and effect of γ-butyrolactone solvent vapor post-annealing on the performance of a mesoporous perovskite solar cell," *RSC Adv.*, vol. 8, no. 2, pp. 724–731, 2018, doi: 10.1039/C7RA10695E.

[73] K. Penpong, C. Seriwatanachai, A. Naikaew, N. Phuphathanaphong, K. K. S. Thant, L. Srathongsian, *et al.*, "Robust perovskite formation via vacuum thermal annealing for indoor perovskite solar cells," *Sci. Rep.*, vol. 13, no. 1, p. 10933, 2023, doi: 10.1038/s41598-023-37155-4.

[74] Y. Y. Kim, T. Y. Yang, R. Suhonen, A. Kemppainen, K. Hwang, N. J. Jeon, J. Seo, "Roll-to-roll gravure-printed flexible perovskite solar cells using eco-friendly antisolvent bathing with wide processing window," *Nat. Commun.*, vol. 11, no. 1, p. 5146, 2020, doi: 10.1038/s41467-020-18940-5.

[75] P. Apilo, J. Hiltunen, M. Välimäki, S. Heinilehto, R. Sliz, and J. Hast, "Roll-to-roll gravure printing of organic photovoltaic modules—insulation of processing defects by an interfacial layer," *Prog. Photovoltaics Res. Appl.*, vol. 23, no. 7, pp. 918–928, Jul. 2015, doi: https://doi.org/10.1002/pip.2508.

[76] J. Yan, T. J. Savenije, L. Mazzarella, and O. Isabella, "Progress and challenges on scaling up of perovskite solar cell technology," *Sustain. Energy Fuels*, vol. 6, no. 2, pp. 243–266, 2022, doi: 10.1039/D1SE01045J.

[77] H. Yu, X. Liu, Y. Xia, Q. Dong, K. Zhang, Z. Wang, *et al.*, "Room-temperature mixed-solvent-vapor annealing for high performance perovskite solar cells," *J. Mater. Chem. A*, vol. 4, no. 1, pp. 321–326, 2016, doi: 10.1039/C5TA08565A.

[78] X. Zheng, W. Kong, J. Wen, J. Hong, H. Luo, R. Xia, *et al.*, "Solvent engineering for scalable fabrication of perovskite/silicon tandem solar cells in air," *Nat. Commun.*, vol. 15, no. 1, p. 4907, 2024, doi: 10.1038/s41467-024-49351-5.

[79] H. Huang, X. Zhang, W. Zhou, Y. Huang, Z. Zheng, X. Chen, *et al.*, "Interface passivation strategies for high-performance perovskite solar cells using two-dimensional perovskites," *Mater. Chem. Front.*, vol. 8, no. 21, pp. 3528–3557, 2024, doi: 10.1039/D4QM00560K.